THE JOURNAL OF
PHYSICAL CHEMISTRY C

Oligomeric Ruthenium Polypyridyl Dye for Improved Stability of Aqueous Photoelectrochemical Cells

Christopher L. Gray, Pengtao Xu, August J. Rothenberger, Stephen J. Koehler, Elizabeth Elacqua, Bratoljub H. Milosavljevic, and Thomas E. Mallouk*

Cite This: *J. Phys. Chem. C* 2020, 124, 3542−3550

Read Online

ACCESS | Metrics & More | Article Recommendations | Supporting Information

ABSTRACT: Water-splitting dye-sensitized photoelectrochemical cells rely on molecular sensitizers to harvest light energy and drive the catalytic reactions necessary to generate hydrogen and oxygen from water. The desorption of sensitizer molecules from the semiconductor−aqueous electrolyte interface is a significant barrier to the practical implementation of these cells. To address this problem, we synthesized an oligomeric ruthenium dye ([**RuP**]$_n$) that has dramatically improved stability as a photosensitizer for TiO_2 electrodes over the pH range of interest (4−7.8) for DSPECs. Additionally, the efficiency of photoelectrochemical charge separation is known to depend on the rate of cross-surface hole diffusion between dye molecules. The oligomeric dye ([**RuP**]$_n$) shows an order of magnitude faster cross-surface hole diffusion than the commonly used monomeric $[Ru(bpy)_2(4,4\text{-}PO_3H_2)_2bpy]^{2+}$ (**RuP**) sensitizer. The enhanced stability of the polymeric dye also enables the use of intensity-modulated photovoltage spectroscopy to measure the recombination rate of photogenerated electrons and holes as a function of electrolyte pH.

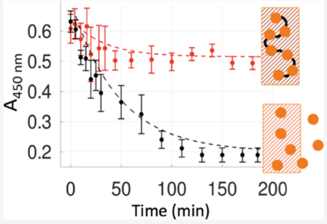

■ INTRODUCTION

Over the next several decades, energy requirements for the human population are expected to double as a result of population and economic growth.[3,4] The storage of renewable energy in the form of hydrogen and liquid fuels will be an important factor in preventing the rise of atmospheric carbon dioxide emissions. One potential method for renewable generation of hydrogen is through the solar-driven electrochemical splitting of water. Water-splitting dye-sensitized photo-electrochemical cells (WS-DSPECs) employ molecular sensitizers to harvest the energy needed to split water into hydrogen and oxygen. The basic electron transfer scheme of a WS-DSPEC is shown in Figure 1. Upon light absorption by a surface-bound sensitizer, a photoexcited electron is injected into the conduction band of an oxide semiconductor such as TiO_2 or SnO_2. The photogenerated electrons are transported through an external circuit to a cathode, where they can be used to reduce water and form hydrogen gas. As electrons are transported through the semiconductor to the electrode back contact, hole diffusion occurs along the surface between dye molecules in order to bring oxidizing equivalents to oxygen-evolving catalyst molecules or nanoparticles. WS-DSPECs are essentially aqueous dye-sensitized solar cells (DSSCs) in which the anode is coupled to a water oxidation catalyst. However, while DSSCs have been optimized extensively and can reach power conversion efficiencies above 15%, WS-DSPECs have struggled to break 1% efficiency.[4] The kinetically demanding water oxidation reaction is slow, making electron−hole recombination the dominant kinetic process, and the aqueous electrolyte introduces stability issues that are much less pronounced in DSSCs. In order to generate one oxygen molecule from water, four oxidizing equivalents (holes) must be transferred to the catalyst from the excited dye molecules. Depending on the architecture of the photoanode (porosity, dye loading, catalyst loading, etc), only dye molecules within a certain distance of catalytic sites can transfer oxidizing equivalents to the catalyst before they are lost to recombina-

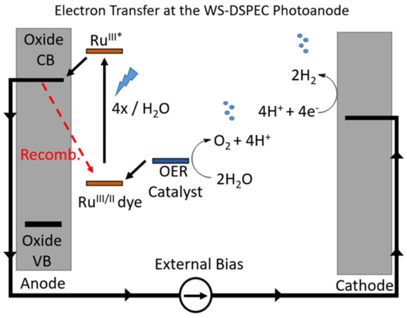

Figure 1. Simplified electron transfer scheme of a WS-DSPEC. Upon light absorption by a surface-bound sensitizer, a photoexcited electron is injected into the conduction band of an oxide semiconductor. Electrons are driven through an external circuit to a cathode, where they reduce water to hydrogen.

Received: January 17, 2020
Published: January 23, 2020

https://dx.doi.org/10.1021/acs.jpcc.0c00493
J. Phys. Chem. C 2020, 124, 3542−3550

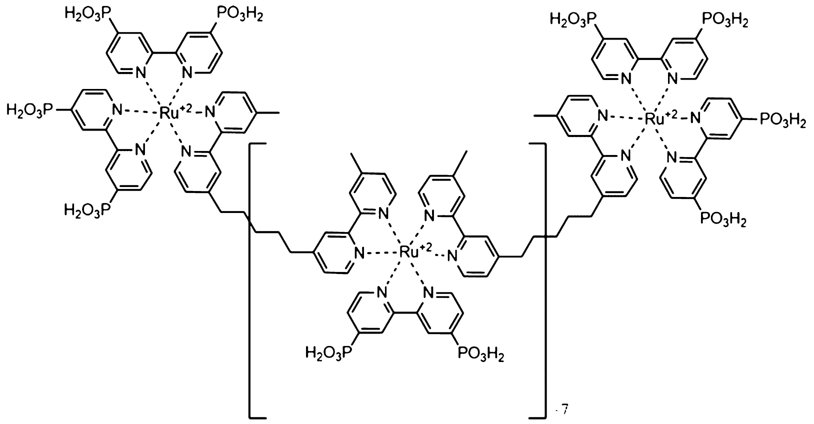

Figure 2. Structure of the oligomeric sensitizer ([**RuP**]$_n$).

Scheme 1. Synthesis of Oligomeric [RuP]$_n$

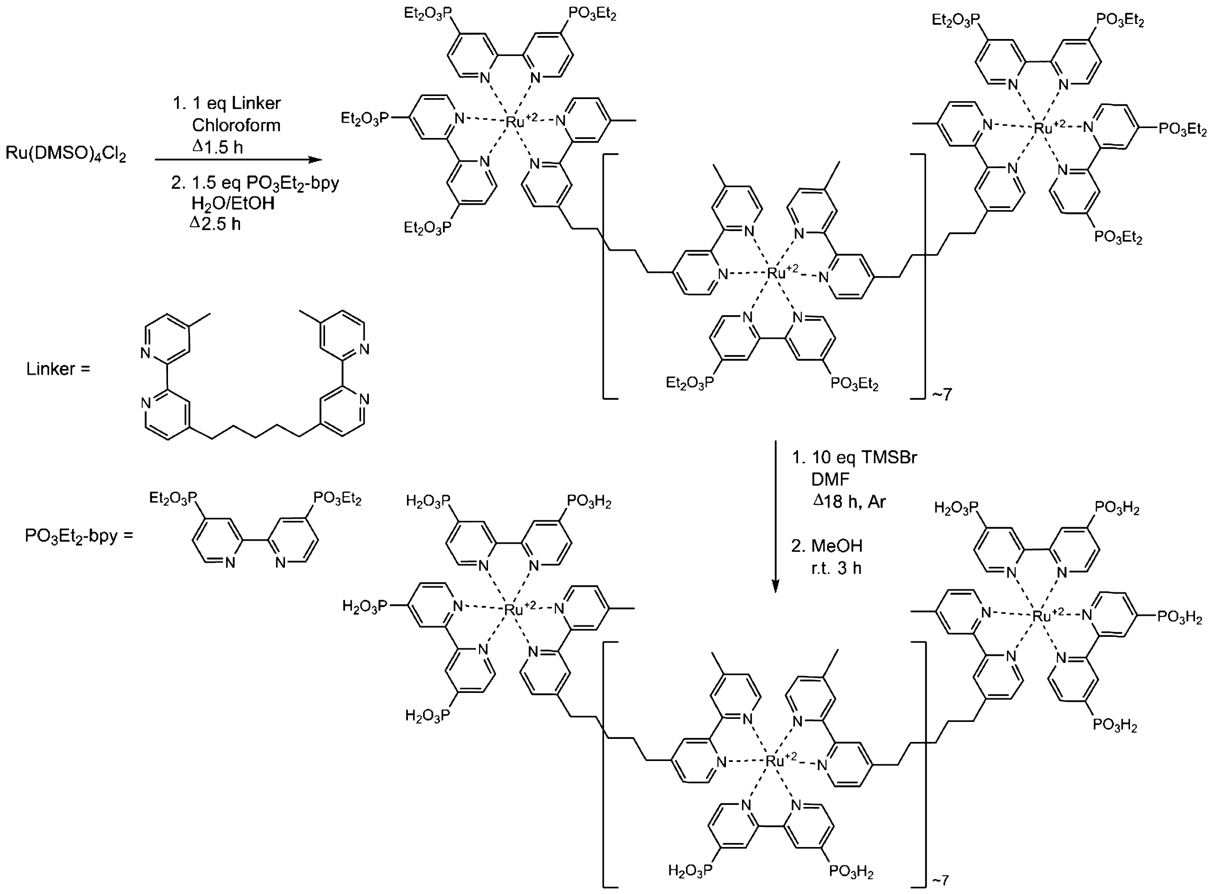

tion. DSSCs can also utilize a broad range of dyes that can be optimized for light absorption and power generation. In contrast, WS-DSPECs are run under aqueous conditions, limiting the choice of dyes to those that have sufficient oxidizing power to generate oxygen from water and requiring surface anchoring groups that resist hydrolysis. Previous studies of WS-DSPECs have primarily utilized a derivative of tris(2,2′-bipyridine)ruthenium(II) with a pair of phosphonate anchoring groups at the 4,4′ position of one bipyridine ligand, $[Ru(bpy)_2(4,4\text{-}PO_3H_2)_2bpy]^{2+}$ (**RuP**),[4−6] although some experiments have also been carried out with porphyrin[7] and perylene diimide[8] sensitizers. Despite the superior stability of the phosphonate anchoring group, dye desorption from the electrode surface is widely recognized as a factor that compromises the stability of WS-DSPECs.[4,5,9]

Much of the literature discusses these cells within the simplification of one-dimensional electron transfer without the kinetic complexity of three-dimensional surface electron exchange rates. Ruthenium centers that are distant from catalytic sites can contribute oxidizing equivalents to the catalyst through a cross-surface hole-hopping mechanism between ruthenium centers. Recent work has identified this cross-surface hole diffusion as one of the limiting factors in the catalytic turnover of these cells.[1,2,10] In particular, it has been shown that each catalytic site effectively draws holes from the dye on the same 20 nm nanoparticle, while most of the dye-

https://dx.doi.org/10.1021/acs.jpcc.0c00493
J. Phys. Chem. C 2020, 124, 3542−3550

coated surface does not contribute to the catalytic cycle.[1] To improve the surface electroactivity, it is necessary to create dyes that have higher hole diffusion constants (Figure 2).

Many groups have attempted to exploit the increased stability of polymers to improve DSSCs[11] and WS-DSPECs. Research groups have attempted deposition of polymeric dyes[12] or polymerized dyes after deposition[13−15] or encased surface-adsorbed dyes in a polymer overlayer[16,17] or a metal oxide shell.[6,18−20] Most of these strategies increase the stability but involve some kind of detrimental trade off. The hole diffusion constant has been shown to be largely determined by the distance between sensitizer molecules. With an oligomeric dye, the light-absorbing moieties are covalently linked before deposition and thereby guaranteed to be at a certain distance from each other on the surface, allowing for holes to be transferred faster between individual dye complexes. This should result in an increase in the hole diffusion constant. The phosphonate anchoring groups increased the stability while lowering the efficiency of electron injection into TiO_2. Recently, injection efficiency has also been identified as a significant bottleneck in these cells.[9,21] Many groups have searched for a water-stable dye that also has a high injection efficiency. The most promising of these are hydroxamate anchoring groups.[4,9] Although previous research has demonstrated that organic dyes can be anchored to TiO_2 electrodes by hydroxamate groups,[22] so far, there are no reports of $Ru(bpy)_3$ analogues.[23,24] The search for a stable dye that has a high quantum yield for charge injection into TiO_2 under aqueous conditions is ongoing. Currently, **RuP** represents one of the best balances of injection efficiency and stability.

In this study, we synthesized a phosphonated oligomeric ruthenium dye ($[\mathbf{RuP}]_n$) that has dramatically improved electrode adhesion from pH 4 to pH 7.8. We measured the long-term stability of the $[\mathbf{RuP}]_n$ sensitizer at higher pH values that are ordinarily incompatible with WS-DSPECs. We also determined the apparent hole diffusion constant of the oligomeric dye. These two dye properties have received recent attention as key limiting factors in the efficiency of WS-DSPECs. The stability over a broad range of pH has enabled us to measure the recombination rate at a higher range of pH for the first time. In addition, the oligomer attains injection yields similar to that of the monomeric **RuP** sensitizer. These results demonstrate that oligomeric dyes are an effective strategy in designing high-stability chromophores for WS-DSPECs (Scheme 1).

■ EXPERIMENTAL SECTION

The 4,4′-bis(diethylphosphonate)-2,2′-bipyridine ligand, $(4,4\text{-}PO_3Et_2)_2bpy$, was purchased from Carbosynth and used without further purification. Bis(2,2-bipyridine)(4,4-diphosphonato-2,2-bipyridine)-ruthenium bromide, $[Ru(bpy)_2(4,4\text{-}PO_3H_2)_2bpy]^{2+}$ (**RuP**), was prepared according to the methods mentioned in the literature.[25]

Synthesis of the Oligomeric Dye ($[\mathbf{RuP}]_n$). Dichlorotetrakis(dimethyl sulfoxide)ruthenium(II)[26] and 1,5-bis-(4-methyl-2,2-bipyridyl-4-yl)pentane were prepared according to the methods mentioned in the literature,[27,28] and the latter was purified by recrystallization from hot *t*-butyl methyl ketone. A portion of $Ru(DMSO)_4Cl_2$ (0.20 g, 0.40 mmol) and 1,5-bis(4-methyl-2,2-bipyridyl-4-yl)pentane (0.17 g, 0.40 mmol) were combined with 50 mL of chloroform and refluxed under argon for 1.5 h. The solvent was removed under reduced pressure to yield dark brown oil. The oil was dissolved in a mixture of 10 mL of H_2O/15 mL of ethanol. A portion of $(4,4\text{-}PO_3Et_2)_2bpy$ (0.10 g, 0.64 mmol) was added, and the solution was refluxed for 2.5 h. A clear, dark red solution resulted. The solvent was reduced to about 10 mL under reduced pressure, and the product was precipitated by addition of aqueous ammonium hexafluorophosphate. The precipitate was filtered and washed with H_2O and diethyl ether to yield a dark red powder (0.29 g, 78%).

In the same manner as the monomer dye (**RuP**), the ethyl ester groups were hydrolyzed by reacting with excess TMS-Br.[25] As has been done for similar oligomer complexes,[28] the degree of polymerization was determined from ^1H NMR experiments by assuming that the end groups contained two phosphonated-2,2-bipyridine units and the interior Ru^{2+} centers had one. The degree of polymerization can then be calculated from the ratio between the average peak areas for the 1,5-bis(4-methyl-2,2′-bipyridyl-4-yl)pentane units and phosphonated-2,2′-bipyridine units. The average degree of polymerization determined by this method was ca. 7 ruthenium centers. MALDI-TOF and ESI mass spectrometry were run on oligomer samples but chains longer than three ruthenium units did not result in a detectable signal. The details and results are given in the Supporting Information. Gel permeation chromatography (GPC) was run on the ethyl-ester-protected oligomeric ruthenium polypyridyl product in chloroform using polystyrene standards. The resulting chromatogram showed oligomeric chain lengths ranging up to 35,000. Taking into account the entire sample volume and oligomers detected by GPC, the overall dispersity ($Đ_M$) was 3.48; however, all constituent peaks comprised a narrow dispersity ($Đ = 1.00−1.02$). Discrete signals corresponding to dimers and trimers represented 23.4 and 6.5% of the sample, respectively, whereas a heptamer peak could be observed that constitutes 41.3% of the sample. Intermediate length oligomers ($10,000 < M_n < 20,000$) comprise approximately 3.9% of the sample. The longer chains ($M_n > 30,000$), which comprise the remaining 24.8% of the sample, are unlikely to penetrate into the electrode pore network. Taking into account the spread of oligomers ranging from 2 to 10 units long in the structure, the sample dispersity is 1.56, similar to what might be expected from supramolecular polymerization that is likely both concentration- and solubility-limited. Further discussion of the GPC data is included in the Supporting Information section.

Photoanode Preparation. All electrodes were prepared on 18 Ω/cm^2 fluorine-doped tin oxide-coated glass (FTO-glass, Hartford Glass Company). A colloidal suspension of anatase TiO_2, prepared as previously described,[1,29] was deposited onto the FTO-glass via the doctor blade method to form 1 cm^2 area. Layers of transparent tape were used to control the thickness of the suspension that was applied to the electrodes. The resulting films were sintered at 300 °C for 20 min, 350 °C for 10 min, and 500 °C for 30 min. For one and two pieces of the tape, the thickness of the films was measured to be approximately 3 and 6 μm, respectively, by profilometry.

All electrodes were sensitized by soaking in 2 mL of 100 μM of the sensitizer (**RuP** or $[\mathbf{RuP}]_n$) in ethanol overnight at room temperature in the dark and then rinsed thoroughly with ethanol and dried under a stream of N_2. Following dye deposition, electrodes were kept in the dark until use.

Insulated silver-plated copper wire was attached to the electrode using silver paste (DuPont CP4922N-100), and contacts were protected using white epoxy (Loctite 1C Hysol).

Before sensitization with dye, TiO_2 film electrodes used in intensity-modulated photovoltage spectroscopy (IMVS) experiments were treated with $TiCl_4$ as described previously.[29]

Electrochemical Measurements. All photoelectrochemical measurements were carried out using an Autolab potentiostat (PGSTAT128N) in a three-electrode electrochemical cell with a Pt wire as the counter electrode and an Ag/AgCl (3 M NaCl) electrode as the reference electrode. Cyclic voltammetry (CV) was conducted on dye-sensitized TiO_2/FTO working electrodes with a platinum wire counter electrode and a Ag/AgCl reference electrode (BASi, MF-2079). CV was performed in 0.1 M $HClO_4$ aqueous solutions at a scan rate of 1 mV/s. The slow scan rate was used to minimize the peak-to-peak separation, which was typically 100 mV as a result of the series resistance of the TiO_2 layers.

Photophysical Measurements. Absorption spectra of the monomer and oligomer were collected in ethanol solutions. Steady-state emission data were collected at room temperature on a custom-built fluorimeter. For steady-state experiments, samples were excited using a light output from a housed 450 W Xe lamp. Sensitizer solutions were freshly prepared in ethanol at 100 μM concentration, added to quartz cuvettes, and bubbled with nitrogen for 20 min. Emission studies conducted on sensitized electrodes were performed in argon-purged acetate buffer (pH = 4.8).

Intensity-Modulated Photovoltage Spectroscopy. A 470 nm LED light (LDC470, Metrohm) provided illumination. The light intensity modulation was realized through an Autolab LED driver controlled by the potentiostat with the ac amplitude set to 10% of the dc level. The dc light intensity was 4.1 mW/cm^2 (470 nm). The applied frequency ranged from 2000 to 1 Hz. The electrolyte was aqueous 0.1 M sodium acetate/acetic acid (pH 4.8) or 0.1 M sodium phosphate buffer (pH 5.8 or 6.8). Four electrodes were run at each pH. Each sample was repeated three times at each intensity, and the results averaged together.

Cross-Surface Electron Diffusion Constant (D_{app}). Following the method of Hanson et al.,[1,5] D_{app} was measured in 0.1 M $HClO_{4(aq)}$ by applying a potential of 2.0 V versus Ag/AgCl (3.5 M NaCl) for 5 min and then 0.0 V for an additional 5 min. D_{app} was calculated by monitoring the change in absorbance at 450 nm and then analyzing the data according to eq 1

$$\Delta A = \frac{2A_{\max} D_{app}{}^{1/2} t^{1/2}}{d\pi^{1/2}} \tag{1}$$

where ΔA is the change in absorbance $[A_{\max} - A(t)]$, $A_{\max}$ is the initial absorbance of the fully reduced film, t is the time in seconds, and d is the thickness of the film (6 μm). The film thickness was acquired from profilometry. D_{app} was determined by fitting the change in absorbance to eq 1 over the linear portion of the experimental data.

Photostability Measurements. The long-term photostability of the adsorbed sensitizer molecules was evaluated using a technique developed by Meyer and co-workers.[5] Briefly, the electrode was subjected to steady-state irradiation under open-circuit conditions. The light from a high-power blue LED (455 nm, fwhm 30 nm, 475 mW/cm^2, Thorlabs, Inc., M455L2) powered by a T-Cube LED driver (Thorlabs, Inc., LEDD1B) was directed onto the sensitized electrodes placed at 45° in a standard 10 mm path length cuvette containing 5 mL of the solutions of interest. The incident light intensity was measured using a thermopile detector (Newport Corp 1918-C meter and 818P-020-12 detector). The absorbance of the electrodes was measured to determine the amount of dye coated every 5 min over the first hour and every 15 min throughout the remainder of the experiment. The electrodes were rinsed with water between each measurement.

RESULTS AND DISCUSSION

A phosphonated oligomeric ruthenium tris(bipyridyl) dye ($[\mathbf{RuP}]_n$) in which the individual $Ru(bpy)_3$ centers are linked by a five-carbon aliphatic chain was synthesized and studied as a sensitizer for TiO_2 photoanodes. Because a relatively long saturated hydrocarbon linker separates the $Ru(bpy)_3$ units, we should expect them to be electronically isolated and to have similar electrochemical and spectroscopic properties to the monomeric sensitizer **RuP**. Some differences between the oligomer and monomer could, however, result from the phosphonate and alkyl substituents that are present on the bpy units within and at the ends of the oligomer chains. We confirmed that the properties of the oligomer are similar to those of **RuP** using CV and steady-state absorption and emission spectroscopy.

Electrochemistry. The electrochemical properties of the oligomer were investigated by CV of the sensitizers adsorbed onto TiO_2 electrodes. CV was carried out on sensitizers on electrodes as these potentials provide the most relevant estimate of the working conditions of a WS-DSPEC.[30] When these $Ru(bpy)_3$ derivatives were anchored to the electrodes, their potentials typically varied by no more than 50 mV.[30] Solubility issues with the electrolyte salts prevented us from carrying out CV on $[\mathbf{RuP}]_n$ in solution. Addition of lithium perchlorate or tetrabutylammonium hexafluorophosphate caused agglomeration and precipitation of the oligomer from solution. The results of CV on sensitized electrodes are shown in Figure 3 and summarized in Table 1. The quasi-reversible

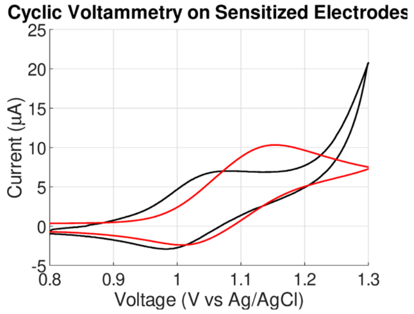

Figure 3. CV of TiO_2 films sensitized with monomeric **RuP** (black) and oligomeric $[\mathbf{RuP}]_n$ (red) dyes in 0.1 M $HClO_4$ electrolyte vs an Ag/AgCl reference electrode at a scan rate of 1 mV/s.

Table 1. Estimated Ground- and Excited-State Redox Properties of RuP and $[\mathbf{RuP}]_n$ on TiO_2 and ZrO_2 Electrodes in Aqueous 0.1 M $HClO_4$

complex	$E_{1/2}(\mathrm{Ru^{III/II}})$ (V)[a]	ΔG_{es} (eV)[b]	$E^*_{1/2}(\mathrm{Ru^{III/II}})$ (V)[c]
monomer (**RuP**)	1.08	1.88[d]	−0.80
oligomer ($[\mathbf{RuP}]_n$)	1.04	1.88[d]	−0.84

[a] From CV measurements on TiO_2 versus Ag/AgCl ref. electrode. [b] From fitting of the emission spectrum on ZrO_2. [c] Calculated from eq 2. [d] Literature value for the monomer from the report by Hanson et al.[30]

($Ru^{III/II}$) potential of the oligomer was observed to be $E_{1/2}$ = 1.04 V versus Ag/AgCl (0.197 V vs NHE). It has been shown that the electron-withdrawing substituent effect of the two PO_3H_2 groups at the 4,4′-bpy positions results in an incremental positive shift in $E_{1/2}(Ru^{III/II})$ of 0.05 V relative to unsubstituted $Ru(bpy)_3$.[30] Conversely, two electron-donating methyl groups result in an incremental negative shift of approximately 0.04 V.[30] Assuming an average oligomer chain length of 7 units, the ratio of phosphonated ligands to alkylated ligands is approximately 4:5. This ratio results in the substituent effects nearly balancing each other out. The resulting $E_{1/2}(Ru^{III/II})$ of the oligomer is 1.04 V compared to the monomer value of $E_{1/2}(Ru^{III/II})$ = 1.08 V.

Steady-State Spectra. The absorption and emission spectra of the monomer and oligomer in methanol solutions are shown in Figure 4. The absorbance maxima of both the oligomer and monomer in solution are 458 nm. Emission spectra were collected for the monomer and oligomer anchored to 5 μm ZrO_2 particles suspended in aqueous 0.1 M $HClO_4$ and are shown in Figure 4. The conduction band potential of ZrO_2 is too negative for either complex to inject an electron from the excited state,[30] so strong emission can be observed. The emission maxima for the adsorbed oligomer and monomer are 654 and 656 nm, respectively. Excited-state reduction potential (E^*_{red}) can be estimated from $E_{red}(Ru(bpy)^{3+/2+})$, and the free energy of emission (ΔG_{es}) using the relationship is given in eq 2, where n = 1 and F is Faraday's constant.

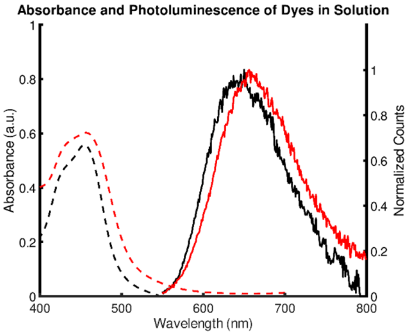

Figure 4. Absorbance (dashed lines) of dyes in methanol and steady-state luminescence (solid lines) of the monomer (black) and oligomer (red) on ZrO_2 powder in aqueous 0.1 M $HClO_4$ solution.

$$E^*_{red} \approx E_{red}(Ru(bpy)^{3+/2+}) - \Delta G_{es}/nF \qquad (2)$$

Given that the oligomer emission maximum is blue-shifted by only a few nm, the literature value of ΔG_{es} for **RuP** was used to estimate the excited-state reduction potential of the oligomer (Table 1). The excited-state reduction potential (E^*_{red}) of the oligomer was estimated to be −0.84 V, according to eq 2.[30] This is about 40 mV more negative than the corresponding monomer excited-state potential (E^*_{red} = −0.88). These experiments show that the ground- and excited-state reduction potentials of the oligomer are slightly more negative than those of the monomeric dye, reflecting the greater degree of alkyl substitution of bpy ligands in the oligomer.

Dye Aggregation. Dye aggregation or multilayer adsorption on the electrode surface is always a concern with dye-sensitized electrodes, especially with polymeric sensitizers. Because some of the dye molecules in aggregates are not directly adsorbed on the oxide surface, the injection yield and, therefore, the cell efficiency are lowered.[31,32] To confirm the absence of aggregation, steady-state luminescence spectra were collected from dye samples in solution and adsorbed on TiO_2 electrodes. When $Ru(bpy)_3$ derivatives are covalently anchored to the semiconducting TiO_2 electrode, the excited state is rapidly quenched through electron injection into the conduction band.[30] We find (Figure 5) that both the monomeric and oligomeric sensitizers exhibit similar weak luminescence when adsorbed to TiO_2 electrodes, indicating similar electron injection kinetics. These results imply that the majority of monomer units in the oligomer chains are adsorbed directly at the TiO_2 surface through their phosphonate anchoring groups.

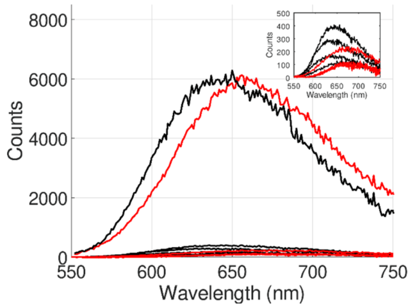

Figure 5. Steady-state emission of monomeric **RuP** (black) and oligomeric $[\mathbf{RuP}]_n$ (red) sensitizers adsorbed to ZrO_2 powder and to TiO_2 electrodes. The inset shows the dye-TiO_2 spectra on an expanded scale.

Pore Penetration. A possible concern with a polymeric sensitizer is its ability to penetrate into the pore network of a thick nanocrystalline TiO_2 photoanode. The pore diameter in dye cell TiO_2 films is generally in the order of 20 nm, and because the monomeric dye has a radius of 1.1 nm,[1] it can readily penetrate the pore network to uniformly sensitize the TiO_2 surface. Because the average length of the oligomer is 7 monomer units, we can estimate its persistence length to be in the range of 2−3 nm, which is still much smaller than the average pore diameter. To confirm that the oligomer dye penetrated fully into the pore network, electrodes were sensitized with oligomers and subsequently sensitized with monomers. The resulting electrodes showed on average less than 1% increase in absorbance after the second sensitization step. This result supports the idea that after the oligomer adsorption step, there is little free area of the electrode available for the smaller **RuP** to adsorb. Cross-sectional energy-dispersive X-ray spectroscopy was also attempted to determine the distribution of Ru atoms in the electrode film, but the dye loading was below the instrument's detection limit.

Photostability in pH 7.8 Phosphate Buffer. Dye-sensitized electrodes were placed in sodium phosphate buffer (pH 7.8) and illuminated with constant irradiation under open-circuit conditions for 4 h. The results are displayed in Figure 6. As observed in other groups,[5,33] the MLCT absorbance of monomer-sensitized electrodes decreased rapidly as a result of dye desorption. By the end of the 3 h experiment, the monomer (**RuP**) had desorbed from the surface and the absorbance reached the baseline of the unfunctionalized TiO_2 layer. Under the same conditions, the oligomer-sensitized electrodes showed a ∼15% drop in absorbance over the first 30 min and were then stable for the 3 h duration of the experiment. This result has profound

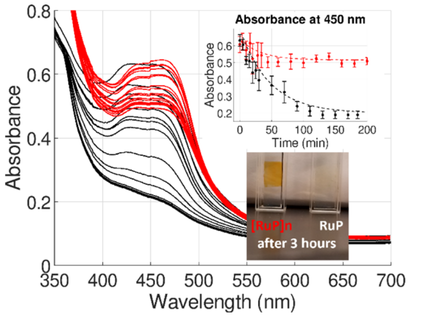

Figure 6. Changes in the absorption spectrum vs time of $[\mathbf{RuP}]_n$ (red) and **RuP** (black) adsorbed on TiO_2 electrodes. Electrodes were held at open circuit in 0.1 M sodium phosphate buffer (pH = 7.8) with constant irradiation (475 mW/cm^2). Inset A: Absorbance changes at 450 nm as a function of time. Inset B: Photographs of electrodes after 3 h.

implications for the incorporation of the oligomer into WS-PECs. First, the oligomer remains absorbed for significantly longer than the monomer at pH 4.8, where WS-DSPECs are studied in order to minimize dye desorption. Second, the oligomer is persistently adsorbed at higher pH (7.8), where the highest efficiency cells have been reported[34] but where the monomer desorbs very rapidly. This dramatically broadens the pH range at which WS-DSPECs can be studied and the types of experiments that can be done. In particular, it opens up opportunities to study these cells as a function of pH. We exploit this property to use transient electrochemical techniques to investigate the kinetics of cross-surface hole transfer and charge recombination from TiO_2 to the oxidized dye molecules as a function of solution pH.

Cross-Surface Hole Transfer. In WS-DSPECs, charge transfer diffusion between oxidized and reduced sensitizer molecules is an important process in connecting the photo-induced charge transfer and catalytic water oxidation steps. The apparent charge transfer diffusion coefficient, D_{app}, was measured for TiO_2 films sensitized with ethanol solutions of **RuP** and $[\mathbf{RuP}]_n$. Spectroelectrochemical absorbance data for a typical oligomer-sensitized electrode are shown in Figure 7.

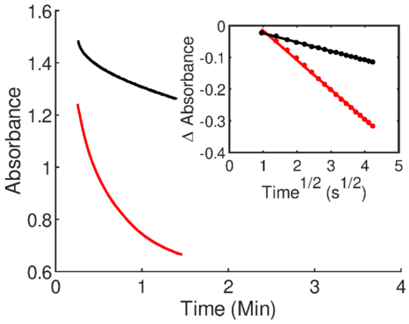

Figure 7. Representative set of spectroelectrochemical absorbance−time data used to calculate D_{app} values for $[\mathbf{RuP}]_n$ (red) and **RuP** (black). Fits to eq 1 are shown in the inset.

The inset shows the linear regression. D_{app} for the oligomer and monomer was found to be $28.1 \pm 1.6 \times 10^{-10}$ and $1.79 \pm 0.58 \times 10^{-10}$ cm^2/s, respectively. The monomer values are in good agreement with literature values for the monomer deposited from ethanol.[1] By covalently linking the oligomer units together, the hole diffusion constant is increased by an order of magnitude relative to the monomer. It has also been shown that an order of magnitude increase in D_{app} can be obtained by depositing the monomer from aqueous 0.1 M $HClO_4$.[1,5] However, our group has shown that acidic depositions negatively affect the overall performance of the electrodes.[1,35] The oligomer is not soluble in aqueous $HClO_4$ solutions, so it was not possible to compare the monomer and oligomer from acidic deposition solutions. Nevertheless, the oligomer displays significant improvement over the monomer, while avoiding the complications of acidic deposition solutions. In the case of the oligomer, it is also possible that hole transfer within the chains is fast relative to D_{app}, which is likely limited by hole transfer between chains adsorbed on the electrode surface.

Intensity-Modulated Photovoltage Spectroscopy. IMVS has been used to measure the recombination kinetics in DSSCs[36,37] and more recently in WS-DSPECs, where charge recombination is typically the dominant kinetic process.[29] Dempsey and co-workers[38] have used transient absorbance techniques to study the recombination dynamics of **RuP** anchored to TiO_2 from pH 1−5 and saw that the recombination rate decreased as pH increased. As we have discussed elsewhere,[29] recombination rates measured by transient absorbance—where high intensity laser excitation is used—are typically much faster than those measured under lower fluence. This is a consequence of the bimolecular nature of the recombination process. Thus it is of interest to compare the kinetics at different pH values using IMVS, which operates under conditions closer to solar fluence.

Details of the IMVS experiments are given in the Supporting Information, and the results are shown in Figures 8 and 9.

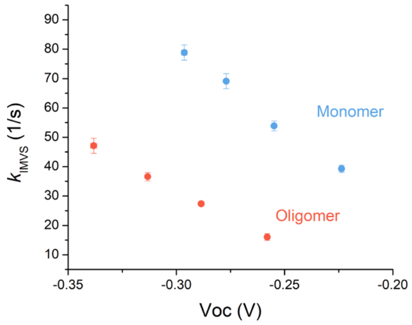

Figure 8. Plots at pH 4.8 of the recombination rate (k_{IMVS}) of the monomer and oligomer as a function of open-circuit photovoltage (V_{oc}).

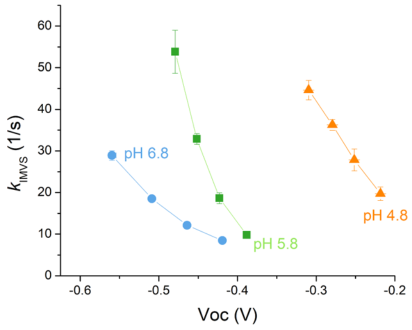

Figure 9. Combined plot of the recombination rate (k_{IMVS}) as a function of open-circuit photovoltage (V_{oc}) for oligomer samples at various pH ranging from 4.8 to 6.8.

Nanocrystalline TiO_2 electrodes were surface passivated by reaction with $TiCl_4$ solution to minimize the surface trap density[29] and were then sensitized with monomeric and oligomeric dyes. IMVS experiments were performed at an open circuit in acetate buffer solutions (pH = 4.8) and the dc light intensity was varied in order to span a range of open-circuit potentials, V_{oc}. Figure 8 shows that the recombination rates increase at more cathodic potentials, which, under open-circuit conditions, represent electrons in higher energy levels at higher light intensities. At pH 4.8, the oligomer has a lower recombination rate than the monomer, possibly because faster hole diffusion results in a longer electron−hole separation distance. IMVS data from oligomer-sensitized electrodes were also obtained in sodium phosphate buffer solutions at pH 5.8 and 6.8. These phosphate buffer solutions were employed to demonstrate the higher pH that these cells could run at if a more adhesive sensitizer was employed. Operating WS-DSPECs in more basic solutions has three different effects, which are difficult to quantify with dyes that adsorb at higher pH. Because the water oxidation potential shifts cathodically with increasing pH, the WS-DSPECs has a larger driving force for oxidizing water, as demonstrated by Gao et al.[34] and by Meyer and coworkers.[39] At the same time, the TiO_2 flat-band potential shifts cathodically with increasing pH, which has two effects: the driving force for electron transfer quenching of the sensitizer excited state decreases, lowering the injection quantum yield, but the negative shift also results in an increase in the open-circuit photovoltage of the cell.

Interestingly, the recombination rates at the same light intensity are smaller as pH increases. This is most likely a result of the decreased electron density which is caused by the decreased efficiency of electron injection. It is well-known that the TiO_2 flat-band potential experiences a cathodic shift as pH increases. As a result of the raised flat-band potential, the injection efficiency for dyes will go down as the pH increases. Despite expecting this trend to continue at a higher pH, there have been no published recombination rates as a function of pH up to pH 7.3 because up until now, there were no dyes that were stable up to this pH.

CONCLUSIONS

Two major limitations of WS-DSPECs are dye desorption and slow cross-surface hole diffusion between oxidized and reduced dye molecules. We have synthesized and characterized an oligomeric ruthenium dye that has significantly faster hole diffusion properties and is persistently adsorbed to high-surface area TiO_2 electrode films over a broader pH range than the commonly employed monomeric sensitizer **RuP**. We provide evidence that the oligomer penetrates into the electrode pores and remains adsorbed under constant illumination and throughout electrochemical experiments such as IMVS. Additionally, the increased stability at higher pH opens up opportunities for incorporating different water oxidation catalysts. IMVS experiments show that the oligomer has a slightly slower recombination rate than the monomer. More interestingly, recombination rates could be measured over a higher pH range for the first time. These measurements show that recombination rates decrease as the pH is increased. It is likely that this is a result of the lower electron injection efficiency at a higher pH. The synthetic method illustrated here could enable the future creation of hybrid oligomers consisting of both phosphonate anchors and carboxylate anchoring groups that could provide a "best of both worlds" solution with both superior adsorption to the electrode and a higher injection efficiency.

ASSOCIATED CONTENT

Supporting Information

The Supporting Information is available free of charge at https://pubs.acs.org/doi/10.1021/acs.jpcc.0c00493.

Details of IMVS analysis, mass spectra, pore penetration studies, and NMR end group analysis (PDF)

AUTHOR INFORMATION

Corresponding Author

Thomas E. Mallouk − *Department of Chemistry, The Pennsylvania State University, University Park, Pennsylvania 16802, United States; Department of Chemistry, University of Pennsylvania, Philadelphia, Pennsylvania 19104, United States;* orcid.org/0000-0003-4599-4208;
Email: mallouk@sas.upenn.edu

Authors

Christopher L. Gray − *Department of Chemistry, The Pennsylvania State University, University Park, Pennsylvania 16802, United States*
Pengtao Xu − *Department of Chemistry, The Pennsylvania State University, University Park, Pennsylvania 16802, United States;* orcid.org/0000-0002-4470-446X
August J. Rothenberger − *Department of Chemistry, The Pennsylvania State University, University Park, Pennsylvania 16802, United States*
Stephen J. Koehler − *Department of Chemistry, The Pennsylvania State University, University Park, Pennsylvania 16802, United States*
Elizabeth Elacqua − *Department of Chemistry, The Pennsylvania State University, University Park, Pennsylvania 16802, United States;* orcid.org/0000-0002-1239-9560
Bratoljub H. Milosavljevic − *Department of Chemistry, The Pennsylvania State University, University Park, Pennsylvania 16802, United States;* orcid.org/0000-0002-6375-1982

Complete contact information is available at:
https://pubs.acs.org/10.1021/acs.jpcc.0c00493

Notes

The authors declare no competing financial interest.

ACKNOWLEDGMENTS

The authors thank Bo Wang for advice on the synthesis of compounds described in this study. This work was supported by the Office of Basic Energy Sciences, Division of Chemical Sciences, Geosciences, and Energy Biosciences, Department of Energy, under contract DE-SC0019781. E.E. and S.J.K. acknowledge startup funds from the Pennsylvania State University for support.

REFERENCES

(1) Swierk, J. R.; McCool, N. S.; Saunders, T. P.; Barber, G. D.; Mallouk, T. E. Effects of Electron Trapping and Protonation on the Efficiency of Water-Splitting Dye-Sensitized Solar Cells. *J. Am. Chem. Soc.* **2014**, *136*, 10974−10982.

(2) Chen, H.-Y.; Ardo, S. Direct Observation of Sequential Oxidations of a Titania-Bound Molecular Proxy Catalyst Generated through Illumination of Molecular Sensitizers. *Nat. Chem.* **2017**, *10*, 17−23.

(3) Lewis, N. S.; Nocera, D. G. Powering the Planet: Chemical Challenges in Solar Energy Utilization. *Proc. Natl. Acad. Sci. U.S.A.* **2006**, *103*, 15729−15735.

(4) Swierk, J. R.; Mallouk, T. E. Design and Development of Photoanodes for Water-Splitting Dye-Sensitized Photoelectrochemical Cells. *Chem. Soc. Rev.* **2013**, *42*, 2357−2387.

(5) Hanson, K.; Brennaman, M. K.; Luo, H.; Glasson, C. R. K.; Concepcion, J. J.; Song, W.; Meyer, T. J. Photostability of Phosphonate-Derivatized, RuII Polypyridyl Complexes on Metal Oxide Surfaces. *ACS Appl. Mater. Interfaces* **2012**, *4*, 1462−1469.

(6) Xu, P.; McCool, N. S.; Mallouk, T. E. Water Splitting Dye-Sensitized Solar Cells. *Nano Today* **2017**, *14*, 42−58.

(7) Moore, G. F.; Blakemore, J. D.; Milot, R. L.; Hull, J. F.; Song, H.-e.; Cai, L.; Schmuttenmaer, C. A.; Crabtree, R. H.; Brudvig, G. W. A Visible Light Water-Splitting Cell with a Photoanode Formed by Codeposition of a High-Potential Porphyrin and an Iridium Water-Oxidation Catalyst. *Energy Environ. Sci.* **2011**, *4*, 2389−2392.

(8) Vagnini, M. T.; Smeigh, A. L.; Blakemore, J. D.; Eaton, S. W.; Schley, N. D.; D'Souza, F.; Crabtree, R. H.; Brudvig, G. W.; Co, D. T.; Wasielewski, M. R. Ultrafast Photodriven Intramolecular Electron Transfer from an Iridium-Based Water-Oxidation Catalyst to Perylene Diimide Derivatives. *Proc. Natl. Acad. Sci. U.S.A.* **2012**, *109*, 15651−15656.

(9) Materna, K. L.; Crabtree, R. H.; Brudvig, G. W. Anchoring Groups for Photocatalytic Water Oxidation on Metal Oxide Surfaces. *Chem. Soc. Rev.* **2017**, *46*, 6099−6110.

(10) Ardo, S.; Meyer, G. J. Direct Observation of Photodriven Intermolecular Hole Transfer across TiO_2 Nanocrystallites: Lateral Self-Exchange Reactions and Catalyst Oxidation. *J. Am. Chem. Soc.* **2010**, *132*, 9283−9285.

(11) Nogueira, A. F.; Longo, C.; De Paoli, M.-A. Polymers in Dye Sensitized Solar Cells: Overview and Perspectives. *Coord. Chem. Rev.* **2004**, *248*, 1455−1468.

(12) Krebs, F. C.; Biancardo, M. Dye Sensitized Photovoltaic Cells: Attaching Conjugated Polymers to Zwitterionic Ruthenium Dyes. *Sol. Energy Mater. Sol. Cells* **2006**, *90*, 142−165.

(13) Lapides, A. M.; Ashford, D. L.; Hanson, K.; Torelli, D. A.; Templeton, J. L.; Meyer, T. J. Stabilization of a Ruthenium(II) Polypyridyl Dye on Nanocrystalline TiO_2 by an Electropolymerized Overlayer. *J. Am. Chem. Soc.* **2013**, *135*, 15450−15458.

(14) Fang, Z.; Keinan, S.; Alibabaei, L.; Luo, H.; Ito, A.; Meyer, T. J. Controlled Electropolymerization of Ruthenium(II) Vinylbipyridyl Complexes in Mesoporous Nanoparticle Films of TiO_2. *Angew. Chem., Int. Ed.* **2014**, *53*, 4872−4876.

(15) Dupray, L. M.; Devenney, M.; Striplin, D. R.; Meyer, T. J. An Antenna Polymer for Visible Energy Transfer. *J. Am. Chem. Soc.* **1997**, *119*, 10243−10244.

(16) Moss, J. A.; Yang, J. C.; Stipkala, J. M.; Wen, X.; Bignozzi, C. A.; Meyer, G. J.; Meyer, T. J. Sensitization and Stabilization of TiO_2 Photoanodes with Electropolymerized Overlayer Films of Ruthenium and Zinc Polypyridyl Complexes: A Stable Aqueous Photoelectrochemical Cell. *Inorg. Chem.* **2004**, *43*, 1784−1792.

(17) Wee, K.-R.; Brennaman, M. K.; Alibabaei, L.; Farnum, B. H.; Sherman, B.; Lapides, A. M.; Meyer, T. J. Stabilization of Ruthenium(II) Polypyridyl Chromophores on Nanoparticle Metal-Oxide Electrodes in Water by Hydrophobic PMMA Overlayers. *J. Am. Chem. Soc.* **2014**, *136*, 13514−13517.

(18) McCool, N. S.; Swierk, J. R.; Nemes, C. T.; Schmuttenmaer, C. A.; Mallouk, T. E. Dynamics of Electron Injection in SnO_2/TiO_2 Core/Shell Electrodes for Water-Splitting Dye-Sensitized Photoelectrochemical Cells. *J. Phys. Chem. Lett.* **2016**, *7*, 2930−2934.

(19) Lee, S.-H. A.; Zhao, Y.; Hernandez-Pagan, E. A.; Blasdel, L.; Youngblood, W. J.; Mallouk, T. E. Electron Transfer Kinetics in Water Splitting Dye-Sensitized Solar Cells Based on Core–Shell Oxide Electrodes. *Faraday Discuss.* **2012**, *155*, 165−176.

(20) Sherman, B. D.; Ashford, D. L.; Lapides, A. M.; Sheridan, M. V.; Wee, K.-R.; Meyer, T. J. Light-Driven Water Splitting with a Molecular Electroassembly-Based Core/Shell Photoanode. *J. Phys. Chem. Lett.* **2015**, *6*, 3213−3217.

(21) Xu, P.; Mallouk, T. E. Charge Transfer Dynamics in Aqueous Dye-Sensitized Photoelectrochemical Cells: Implications for Water Splitting Efficiency. *J. Phys. Chem. C* **2019**, *123*, 299−305.

(22) Koenigsmann, C.; Ripolles, T. S.; Brennan, B. J.; Negre, C. F. A.; Koepf, M.; Durrell, A. C.; Milot, R. L.; Torre, J. A.; Crabtree, R. H.; Batista, V. S.; et al. Substitution of a Hydroxamic Acid Anchor into the MK-2 Dye for Enhanced Photovoltaic Performance and Water Stability in a DSSC. *Phys. Chem. Chem. Phys.* **2014**, *16*, 16629−16641.

(23) McNamara, W. R.; Milot, R. L.; Song, H.-e.; Snoeberger III, R. C., III; Batista, V. S.; Schmuttenmaer, C. A.; Brudvig, G. W.; Crabtree, R. H. Water-Stable, Hydroxamate Anchors for Functionalization of TiO_2 Surfaces with Ultrafast Interfacial Electron Transfer. *Energy Environ. Sci.* **2010**, *3*, 917−923.

(24) Brewster, T. P.; Konezny, S. J.; Sheehan, S. W.; Martini, L. A.; Schmuttenmaer, C. A.; Batista, V. S.; Crabtree, R. H. Hydroxamate Anchors for Improved Photoconversion in Dye-Sensitized Solar Cells. *Inorg. Chem.* **2013**, *52*, 6752−6764.

(25) Gillaizeau-Gauthier, I.; Odobel, F.; Alebbi, M.; Argazzi, R.; Costa, E.; Bignozzi, C. A.; Qu, P.; Meyer, G. J. Phosphonate-Based Bipyridine Dyes for Stable Photovoltaic Devices. *Inorg. Chem.* **2001**, *40*, 6073−6079.

(26) Evans, I. P.; Spencer, A.; Wilkinson, G. Dichlorotetrakis (Dimethyl Sulphoxide) Ruthenium (II) and Its Use as a Source Material for Some New Ruthenium (II) Complexes. *J. Chem. Soc., Dalton Trans.* **1973**, 204−209.

(27) Schmehl, R. H.; Auerbach, R. A.; Wacholtz, W. F.; Elliott, C. M.; Freitag, R. A.; Merkert, J. W. Formation and Photophysical Properties of Iron-Ruthenium Tetranuclear Bipyridyl Complexes of the Type $\{[(Bpy)_2Ru(L\text{-}L)]_3Fe\}$. *Inorg. Chem.* **1986**, *25*, 2440−2445.

(28) Hara, M.; Lean, J. T.; Mallouk, T. E. Photocatalytic Oxidation of Water by Silica-Supported Tris (4, 4'-Dialkyl-2, 2'-Bipyridyl) Ruthenium Polymeric Sensitizers and Colloidal Iridium Oxide. *Chem. Mater.* **2001**, *13*, 4668−4675.

(29) Xu, P.; Gray, C. L.; Xiao, L.; Mallouk, T. E. Charge Recombination with Fractional Reaction Orders in Water-Splitting Dye-Sensitized Photoelectrochemical Cells. *J. Am. Chem. Soc.* **2018**, *140*, 11647−11654.

(30) Hanson, K.; Brennaman, M. K.; Ito, A.; Luo, H.; Song, W.; Parker, K. A.; Ghosh, R.; Norris, M. R.; Glasson, C. R. K.; Concepcion, J. J.; Lopez, R.; Meyer, T. J. Structure−Property Relationships in Phosphonate-Derivatized, RuII Polypyridyl Dyes on Metal Oxide Surfaces in an Aqueous Environment. *J. Phys. Chem. C* **2012**, *116*, 14837−14847.

(31) Matsuzaki, H.; Murakami, T. N.; Masaki, N.; Furube, A.; Kimura, M.; Mori, S. Dye Aggregation Effect on Interfacial Electron-Transfer Dynamics in Zinc Phthalocyanine-Sensitized Solar Cells. *J. Phys. Chem. C* **2014**, *118*, 17205−17212.

(32) Khazraji, A. C.; Hotchandani, S.; Das, S.; Kamat, P. V. Controlling Dye (Merocyanine-540) Aggregation on Nanostructured TiO_2 Films. An Organized Assembly Approach for Enhancing the Efficiency of Photosensitization. *J. Phys. Chem. B* **1999**, *103*, 4693−4700.

(33) Hyde, J. T.; Hanson, K.; Vannucci, A. K.; Lapides, A. M.; Alibabaei, L.; Norris, M. R.; Meyer, T. J.; Harrison, D. P. Electrochemical Instability of Phosphonate-Derivatized, Ruthenium(III) Polypyridyl Complexes on Metal Oxide Surfaces. *ACS Appl. Mater. Interfaces* **2015**, *7*, 9554−9562.

(34) Gao, Y.; Ding, X.; Liu, J.; Wang, L.; Lu, Z.; Li, L.; Sun, L. Visible Light Driven Water Splitting in a Molecular Device with Unprecedentedly High Photocurrent Density. *J. Am. Chem. Soc.* **2013**, *135*, 4219−4222.

(35) McCool, N. S.; Swierk, J. R.; Nemes, C. T.; Saunders, T. P.; Schmuttenmaer, C. A.; Mallouk, T. E. Proton-Induced Trap States, Injection and Recombination Dynamics in Water-Splitting Dye-Sensitized Photoelectrochemical Cells. *ACS Appl. Mater. Interfaces* **2016**, *8*, 16727−16735.

(36) Krüger, J.; Plass, R.; Grätzel, M.; Cameron, P. J.; Peter, L. M. Charge Transport and Back Reaction in Solid-State Dye-Sensitized

Solar Cells: A Study Using Intensity-Modulated Photovoltage and Photocurrent Spectroscopy. *J. Phys. Chem. B* **2003**, *107*, 7536−7539.

(37) Feng, X.; Zhu, K.; Frank, A. J.; Grimes, C. A.; Mallouk, T. E. Rapid Charge Transport in Dye-Sensitized Solar Cells Made from Vertically Aligned Single-Crystal Rutile TiO_2 Nanowires. *Angew. Chem.* **2012**, *124*, 2781−2784.

(38) Knauf, R. R.; Brennaman, M. K.; Alibabaei, L.; Norris, M. R.; Dempsey, J. L. Revealing the Relationship between Semiconductor Electronic Structure and Electron Transfer Dynamics at Metal Oxide−Chromophore Interfaces. *J. Phys. Chem. C* **2013**, *117*, 25259−25268.

(39) Sherman, B. D.; Sheridan, M. V.; Wee, K.-R.; Marquard, S. L.; Wang, D.; Alibabaei, L.; Ashford, D. L.; Meyer, T. J. A Dye-Sensitized Photoelectrochemical Tandem Cell for Light Driven Hydrogen Production from Water. *J. Am. Chem. Soc.* **2016**, *138*, 16745−16753.